DNA Nanotechnology

DOI: 10.1002/anie.201203716

Discovery of the DNA "Genetic Code" for Abiological Gold Nanoparticle Morphologies**

*Zidong Wang, Longhua Tang, Li Huey Tan, Jinghong Li, and Yi Lu**

The elucidation of the three-letter genetic codes, consisting of different combinations of DNA nucleotides, for the synthesis of proteins was a foundation on which modern biology was built. This milestone achievement not only marked how much we understand biology, but also allowed the use of these codes to synthesize new biomolecules with predicted sequences, structures, and functions. DNA is known for its well-defined structures and selective recognition. Because it is highly programmable, DNA has been widely used as a template or scaffold to functionalize and assemble nanomaterials for various applications[1] and the principles of DNA-directed assembly have been summarized.[2] The majority of the work so far, however, has employed functionalization of nanomaterials with DNA following nanomaterial synthesis, thus the DNA was unable to influence the morphology of the nanomaterials. Among the few studies that have used DNA to control the morphology of nanomaterials during their synthesis, there is evidence that different sequences of DNA can influence both the structure and function of nanomaterials, such as silver clusters and quantum dots.[3] However, to our knowledge, no study has comprehensively and systematically reported on the effect of varying DNA sequences on the morphology of nanomaterials. Just as in the case of genetic codes for biomolecular synthesis, elucidating such DNA "codes" that control the synthesis and structure of nanomaterials could have a profound impact on nanotechnology, because of the wide range of applications for nanomaterials with various shapes and structures in catalysis, sensing, imaging, electronics, and medicine.[4]

Recently, we reported that DNA could adsorb onto gold nanospheres and guide their growth into nanoflowers.[3d] However, the true influence of DNA on controlling nanoparticle morphology remains to be explored, and the rules of such control have not been discovered. Thus, we wondered whether different combinations of DNA sequences could constitute a "genetic code" to direct the morphology of nanomaterials. Herein, we report the discovery of a new DNA-encoding scheme for controlling the synthesis of gold nanoparticles with a variety of novel shapes. Furthermore, the underlying rules governing the morphological controls by different DNA molecules and their combinations have been elucidated, and these rules could serve as guidelines for precisely controlled gold nanomaterial synthesis.

Seed-mediated synthesis methods are commonly used to prepare nanocrystals with controlled morphologies.[4c,5] In this approach, preformed seeds are first introduced into a growth solution, where molecular capping agents are usually added to selectively bind to a certain facet, and thus mediate the growth of seeds into different shapes. However, designing effective capping agents to control the evolution of seeds into the desired shapes presents a significant challenge. To explore the effect of different DNA sequences on the metal nanoparticle morphology during seed-mediated synthesis, we chose gold nanoprisms as a model system for further nanomaterial growth. Gold nanoprisms are planar twined crystals, with {111} facets at their top and bottom flat surfaces, and stacking faults on the side faces.[6] Because of these properties, the gold nanoprism is an excellent template to explore controlled growth in both the vertical and horizontal directions.[4b,7]

To search for DNA sequences that can direct the morphology of nanomaterials during their synthesis, purified gold nanoprism seeds were incubated individually with oligo dA_{30} (A30), oligo dT_{30} (T30), oligo dC_{30} (C30), or oligo dG_{20} (G20). G20 was tested instead of G30, because of the difficulty in synthesizing DNA composed of more than 20 G residues. Afterwards, a mild reducing agent, hydroxylamine (NH_2OH), and a gold salt, hydrogen tetrachloroaurate-(III) ($HAuCl_4$), were added to initiate particle growth. The morphologies of the resulting nanoparticles were characterized using scanning electron microscopy (SEM) and transmission electron microscopy (TEM). Interestingly, the nanoparticles resulting from incubation of the nanoprisms with different DNA sequences, all adopted different morphologies with high yields and reproducibility (Figure 1). Nanoparticles synthesized with A30 were round nanoplates with rough

[*] Dr. Z. Wang, L. H. Tan, Prof. Dr. Y. Lu
Department of Materials Science and Engineering, Department of Chemistry, Beckman Institute for Advanced Science and Technology, University of Illinois at Urbana–Champaign
Urbana, IL 61801 (USA)
E-mail: yi-lu@illinois.edu
Homepage: http://www.chemistry.illinois.edu/faculty/Yi_Lu.html
L. Tang, Prof. Dr. J. Li
Department of Chemistry, Beijing Key Laboratory for Analytical Methods and Instrumentation, Key Laboratory of Bioorganic Phosphorus Chemistry & Chemical Biology, Tsinghua University
Beijing, 100084 (China)

[**] We wish to thank Prof. Catherine Murphy for helpful discussions, and Hannah Ihms and Tiffany Hopper for proof-reading the manuscript. This work has been supported by the National Science Foundation Center for Nanoscale Chemical-Electrical-Mechanical Manufacturing Systems (Nano-CEMMS) under NSF Award no. 0749028 (CMMI) and by the National Basic Research Program of China (No. 2011CB935704). Scanning Electron Microscopy was carried out at the Center for Microanalysis of Materials, University of Illinois, which is supported by the U.S. Department of Energy under Grant DEFG02-91-ER45439.

Supporting information for this article (experimental details) is available on the WWW under http://dx.doi.org/10.1002/anie.201203716.

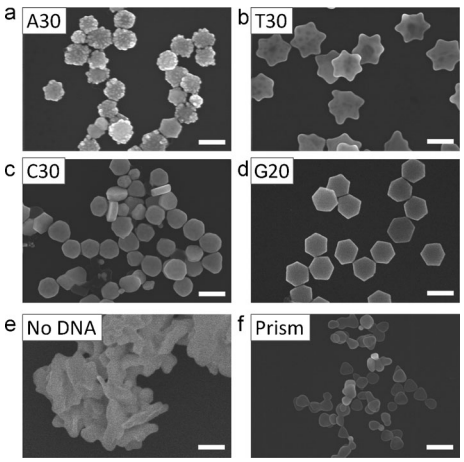

Figure 1. SEM images of the gold nanoparticles synthesized with a) A30, b) T30, c) C30, d) G20, e) in the absence of DNA, or f) in the absence of gold salt. Scale bars = 200 nm.

surfaces (Figure 1 a), whereas nanoparticles with T30 grew into six-pointed nanostars (Figure 1 b). Particles synthesized with C30 formed round nanoplates with smooth surfaces (Figure 1 c), while particles arising from G20 yielded hexagonal nanoplates (Figure 1 d). TEM images of these four types of nanoparticles are shown in the Supporting Information, Figure S1. Gold nanoparticles synthesized with each type of DNA sequence were uniformly shaped and monodisperse. In contrast, when nanoprisms were grown in the absence of DNA under identical conditions, the nanoparticles produced were microsized gold agglomerations and had irregular shapes (Figure 1 e). In addition, if the purified nanoprisms were incubated with DNA in the absence of a reducing agent or gold salts under otherwise identical conditions, minimal changes in the particle morphologies were observed (Figure 1 f). These results strongly suggest that the sequence of the added DNA played a significant role in controlling the morphologies of the nanomaterials during synthesis.

We then investigated the effect of DNA length on nanoparticle synthesis by varying the DNA length from 5–30 bases (or 5–20 bases in the case of oligo dG). As shown in Figure S2, when the length of each type of DNA changed from 5 to 10, and then to 20 bases (for oligo dG) or 30 bases (for oligo dA, oligo dT, and oligo dC), the resulting nanoparticles had similar shapes regardless of the length of the DNA, indicating that it was the DNA sequence, rather than its length, that determined the morphology of the nanoparticles. To further explore this result, we repeated the same experiment using monomeric dAMP, dTMP, dCMP, or dGMP. As shown in Figure S3, each type of deoxyribonucleotide displayed similar morphological effects as compared to its corresponding oligodeoxyribonucleotide, but the nanoparticles synthesized with mononucleotides were much less stable and tended to aggregate much more readily than those synthesized with longer DNA strands. All of these results demonstrated that DNA composed of different sequences could direct the growth of the nanoprism into different shapes, and each type of oligodeoxyribonucleotide encoded the formation of nanoparticles with certain shapes.

To understand this DNA-directed nanoparticle growth and shape control, we monitored the absorbance changes of the nanoparticle solution in the presence of each type of the oligodeoxynucleotides with a UV/Vis-NIR spectrometer. As shown in Figure S4 a and S3 c, for the cases of A20 and C20, the absorbance of the as-synthesized nanoparticle solution was blue-shifted in the first two minutes and subsequently red-shifted back to 800 nm with increasing absorbance intensity. The nanoparticle growth was completed within ten minutes. The absorbance of the sample with G20 also showed an initial blue-shift in the first minute of growth, and then red-shifted with a peak at 950 nm (Figure S4 d). In contrast, for growth solution containing T20, the absorbance increased and the peak at 800 nm was continuously red-shifted over the course of particle growth; the final nanoparticle solution showed a broad peak at 1250 nm (Figure S4 b). This difference in the change in absorbance indicates different pathways for the evolution of nanoparticles grown from different DNA sequences.

To further study this time-dependent shape evolution, nanoparticle growth was halted at different times by adding an excess of mercaptopropionic acid (MPA), the morphologies of the intermediates were then observed using SEM. As shown in Figure S5 a and S5 c, the nanoprisms with A20 or C20 first grew larger into truncated prisms or round nanoplates in the first three minutes, and then horizontal growth slowed down while vertical growth became more prominent. While both A20 and C20 produced thicker particles, A20 induced the formation of round nanoplates with bumpy surfaces and C20 produced round nanoplates with smooth surfaces. On the other hand, the nanoprisms incubated with T20 grew horizontally in the first two minutes into hexagonal plates. Each vertex of the hexagon then sharpened, and the six-pointed nanostars were well formed after ten minutes of particle growth (Figure S5 b). In the case of G20, the nanoprisms first evolved into round nanoplates, and then into nanohexagons within ten minutes (Figure S5 d). These results suggest that DNA acts as template to mediate the evolution of the nanoseeds into different shapes depending on the DNA sequences.

The different morphological effects controlled by specific DNA sequences can be attributed to different interactions of the DNA with gold nanoprism seeds. Several studies have been carried out to understand the nature of interaction of DNA bases or nuclosides with gold surfaces using various analytical methods, such as reflection absoption infrared (RAIR) spectroscopy or surface-enhanced raman spectroscopy (SERS). These studies suggest that the DNA–gold interaction is highly sequence-dependent, and that the purines adsorb on the gold surface more strongly than the pyrimidines, in the order of $G > A > C > T$.[8] The gold nanoprism seeds used in the current study are anisotropic with large planar {111} facets on both the top and bottom surfaces. We believe different DNA bases bind differently with the facets of the gold nanoprism, and direct nanoseeds to grow in different directions, as shown in the kinetics study (Figure S3, S4), resulting in different morphologies.

While it is interesting to find that oligo dA, dT, dC, and dG induce nanoparticles to take on different shapes, we decided to explore this phenomenon in more depth. These oligonucleotides represent the simplest cases of DNA, but most single-stranded DNAs contain more than one type of deoxyribonucleotide. To explore the use of DNA as a coding system to modulate nanoparticle morphology, we extended our investigation to DNA containing two types of deoxyribonucleotides. Because 30 mer DNA had previously been shown to produce nanoparticles with a controlled morphology and good colloidal stability,[3d] we fixed the length of these new DNA strands at 30 nt but divided the nucleotides into two segments. Each segment contained only one type of deoxyribonucleotide; for example, T5G20 (T5G25 was not tested due to synthetic difficulty), T10G20, T15G15, T20G10, and T25G5, for the combination of T and G residues. As shown in Figure S6a, the morpholgies of the nanomaterials synthesized in the presence of T5G20 and T10G20 were similar to those formed in the presence G20. A further increase in the number of T residues (see T20G10 and T25G5) produced six-pointed star-like nanoparticles, similar to those formed in the presence of T30. These results show that T and G residues compete with each other for control of the morphologies, which progress from the nanohexagon prefered by oligo dG to the six-pointed star preferred by oligo dT.

To find out if the above mophology control by the combination of dT and dG also applies to other combinations, we next tested combinations of dA with dG and dC with dG. For the combination of dA and dG, A5G20 and A10G20 produced nanohexogons similar to that of oligo dG (Figure S6b and summarized in Figure 2). However, when the length of the dA segment increased, the edges of the resulting nanohexagon became rough, apparently from competition with the oligo dA (see A15G15). When the length of the oligo dA segment was increased to 20 nt (A20G10) or 25 nt (A25G5), the resulting nanoparticles were round nanoplates with rough surfaces, similar to those formed in the presence of A30. Therefore, the morphological control of dA and dG compete with each other in the combination of dA and dG residues, similar to that of the combination of dT and dG described above. The effects of the combination of dG and dC (see Figure S6c and Figure 2) are also similar, as C10G20 resulted in nanohexagons, in which the effects of dG predominated. As the length of the dC segment increased, round nanoplates with rough surfaces were formed.

To find out if the two nucleotides always compete with each other as in the case of the combinations of dT/dG, dA/dG, and dC/dG, we next examined the effects of a combination of dT and dA. As shown in Figure S6d and Figure 2, nanoparticles grown in the presence of all combinations of dT and dA (T20A10, T15A15, and T10A20) were round nanoplates with rough surfaces, similar to what was observed in the presence of A30 alone and different from that of T30 (Figure 1a). This result suggests that dA always dominates dT in controlling the nanoparticle morphologies when the dA segment length is longer than five bases. A similar phenomenon was observed in combinations of dA and dC, as all tested sequences (A5C25, A10C20, A15C15, A20C10, A25C5)

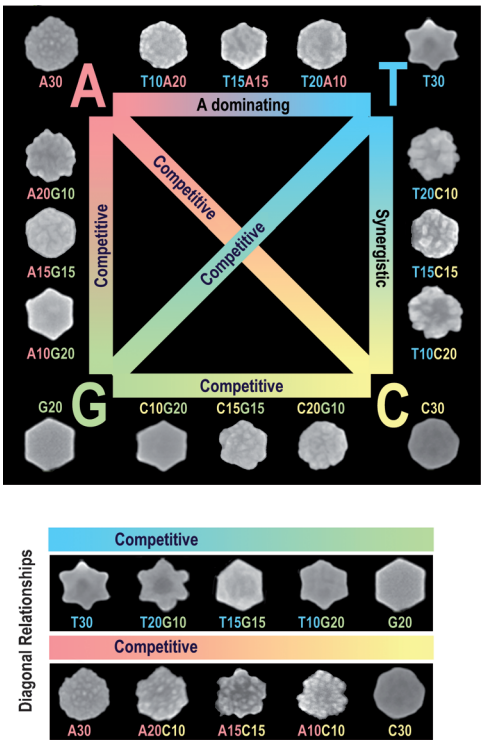

Figure 2. Scheme summarizing the shape-control effects of different DNA sequences and their effects in combination. Representative SEM images of nanoparticles produced by different DNA sequences are shown. Bottom: diagonal relationships between dT and dG and between dA and dC. For complete images of each representative, see Figure S6 in the Supporting Information.

produced round nanoplates with rough surfaces similar to that of A30 alone. The interplay between dA and dC will be further discussed below.

While the above combinations resulted in morphologies that resemble those arising from one type of nucleotide, whether they are equally competitive or one is dominating, the combination of dT and dC causes morphologies that are different from those either oligo dT or oligo dC alone (Figure S6e or Figure 2). All of the DNA sequences tested (T5C25, T10C20, T15C15, T20C10, and T25C5) produced flower-like nanoparticles, with thin central areas and thick edges wrapped with multiple tips. With the increase of dT content, the edges grew thicker and the tips grew longer. Therefore, the morphological effect combinations of dT and dC is synergistic instead of competitive or dominating. By comparing the newly formed nanoparticle morphologies with the morphology of the original nanoprism seeds, the shaping effects of dG, dT, dA, dC in homogenous oligonucleotides or in combination could be identified (and are described in detail in Figure 3). The morphological effects of dG and dT are apparent in the AG, CG, TG, and TC combinations. The rounding effects of dA were confirmed in the AT, AG, and AC combinations. The one exception in these predictions is the case of dC. Even though oligo dC was shown to induce round nanoplates with flat surfaces, once combined with dT or dG, dC induced the formation of rough nanoplates; thus, its

(1) One-base type oligodeoxynucleotides

	Morphological effect
G	Formation of flat nanohexagons
T	Formation of six-pointed nanostars
A	Formation of round rough plates
C	Formation of round flat plates

(2) Two-base type oligodeoxynucleotides

	Shaping effect	Surface effect
G	Hexagon forming	Flattening
T	Six-pointed star forming	Smoothing, edge thickening
A	Rounding	Roughening
C	Rounding	Roughening

Figure 3. Tables summarizing the morphological effects of each type of deoxyribonucleotide on gold nanoparticle formation.

morphological effects were similar to those of dA in combination with other bases.

In addition to summarizing the effects on nanoparticle morphologies by the oligo dG, dT, dA, and dC alone, we have also studied the interplay between the bases by analyzing the effect that the TG, AG, CG, TA, TC, and AC combinations had on nanoparticle formation. In TG, AG, and CG combinations, the morphological influence of each deoxyribonucleotide competed directly with one another, and the longer segment dominated the shaping process (Figure 2). In the AC combinations, since dA and dC have the same morphological effects when combined with another nucleotide, it is difficult to differentiate their interaction, and we assigned it as a competitive interaction for simplicity. The AT combinations were also competitive, but the shaping effect of dA dominated, even if it was shorter than the dT segment. The TC combinations showed a synergistic interaction, producing large petals on the sides of the plates, and creating a morphology distinctly different from either oligo dT or oligo dC (Figure 2).

In summary, we have demonstrated that DNA can be used to control the morphologies of gold nanomaterials during seed-mediated growth. The morphological effects of each deoxyribonucleotide were identified and rules for these effects were summarized. When two deoxyribonucleotides were combined in a single strand and incubated with a developing nanoparticle, two effects (i.e., competitive and synergistic) were observed. With this DNA-encoded nanosynthesis method, a number of nanoparticles with novel shapes were synthesized. Since nanoparticles with complex shapes and rough surfaces have been recently shown to have enhanced performance in SERS, catalysis, and cellular uptake,[4m,9] this work could provide a new method for synthesizing nanoparticles with predictable structures for widespread applications.

Received: May 14, 2012
Revised: June 27, 2012
Published online: August 2, 2012

Keywords: DNA · genetic code · gold · nanoparticles · nanoparticle synthesis

[1] a) C. A. Mirkin, R. L. Letsinger, R. C. Mucic, J. J. Storhoff, *Nature* **1996**, *382*, 607–609; b) A. P. Alivisatos, K. P. Johnsson, X. Peng, T. E. Wilson, C. J. Loweth, M. P. Bruchez, Jr., P. G. Schultz, *Nature* **1996**, *382*, 609–611; c) H. Yan, S. H. Park, G. Finkelstein, J. H. Reif, T. H. LaBean, *Science* **2003**, *301*, 1882–1884; d) N. C. Seeman, *Nature* **2003**, *421*, 427–431; e) P. W. K. Rothemund, *Nature* **2006**, *440*, 297–302; f) J. H. Lee, D. P. Wernette, M. V. Yigit, J. Liu, Z. Wang, Y. Lu, *Angew. Chem.* **2007**, *119*, 9164–9168; *Angew. Chem. Int. Ed.* **2007**, *46*, 9006–9010; g) Y. He, T. Ye, M. Su, C. Zhang, A. E. Ribbe, W. Jiang, C. D. Mao, *Nature* **2008**, *452*, 198–201; h) J. Sharma, R. Chhabra, A. Cheng, J. Brownell, Y. Liu, H. Yan, *Science* **2009**, *323*, 112–116.

[2] a) J. J. Storhoff, C. A. Mirkin, *Chem. Rev.* **1999**, *99*, 1849–1862; b) C. J. Loweth, W. B. Caldwell, X. Peng, A. P. Alivisatos, P. G. Schultz, *Angew. Chem.* **1999**, *111*, 1925–1929; *Angew. Chem. Int. Ed.* **1999**, *38*, 1808–1812; c) Y. Lu, J. W. Liu, *Acc. Chem. Res.* **2007**, *40*, 315–323; d) S. Y. Park, A. K. R. Lytton-Jean, B. Lee, S. Weigand, G. C. Schatz, C. A. Mirkin, *Nature* **2008**, *451*, 553–556; e) D. Nykypanchuk, M. M. Maye, D. van der Lelie, O. Gang, *Nature* **2008**, *451*, 549–552.

[3] a) J. Nowakowski, P. J. Shim, G. S. Prasad, C. D. Stout, G. F. Joyce, *Nat. Struct. Biol.* **1999**, *6*, 151–156; b) Q. B. Wang, Y. Liu, Y. G. Ke, H. Yan, *Angew. Chem.* **2008**, *120*, 322–325; *Angew. Chem. Int. Ed.* **2008**, *47*, 316–319; c) C. I. Richards, S. Choi, J. C. Hsiang, Y. Antoku, T. Vosch, A. Bongiorno, Y. L. Tzeng, R. M. Dickson, *J. Am. Chem. Soc.* **2008**, *130*, 5038–5039; d) Z. D. Wang, J. Q. Zhang, J. M. Ekman, P. J. A. Kenis, Y. Lu, *Nano Lett.* **2010**, *10*, 1886–1891; e) G. Tikhomirov, S. Hoogland, P. E. Lee, A. Fischer, E. H. Sargent, S. O. Kelley, *Nat. Nanotechnol.* **2011**, *6*, 485–490.

[4] a) C. B. Murray, S. H. Sun, H. Doyle, T. Betley, *MRS Bull.* **2001**, *26*, 985–991; b) R. C. Jin, Y. W. Cao, C. A. Mirkin, K. L. Kelly, G. C. Schatz, J. G. Zheng, *Science* **2001**, *294*, 1901–1903; c) N. R. Jana, L. Gearheart, C. J. Murphy, *J. Phys. Chem. B* **2001**, *105*, 4065–4067; d) Y. G. Sun, Y. N. Xia, *Science* **2002**, *298*, 2176–2179; e) J. Liu, Y. Lu, *J. Am. Chem. Soc.* **2003**, *125*, 6642–6643; f) Y. D. Yin, R. M. Rioux, C. K. Erdonmez, S. Hughes, G. A. Somorjai, A. P. Alivisatos, *Science* **2004**, *304*, 711–714; g) M. C. Daniel, D. Astruc, *Chem. Rev.* **2004**, *104*, 293–346; h) C. Sönnichsen, B. M. Reinhard, J. Liphardt, A. P. Alivisatos, *Nat. Biotechnol.* **2005**, *23*, 741–745; i) X. H. Huang, I. H. El-Sayed, W. Qian, M. A. El-Sayed, *J. Am. Chem. Soc.* **2006**, *128*, 2115–2120; j) A. R. Tao, S. Habas, P. D. Yang, *Small* **2008**, *4*, 310–325; k) Z. D. Wang, Y. Lu, *J. Mater. Chem.* **2009**, *19*, 1788–1798; l) Y. Xia, Y. J. Xiong, B. Lim, S. E. Skrabalak, *Angew. Chem.* **2008**, *121*, 62–108; *Angew. Chem. Int. Ed.* **2008**, *48*, 60–103; m) B. Lim, M. J. Jiang, P. H. C. Camargo, E. C. Cho, J. Tao, X. M. Lu, Y. M. Zhu, Y. A. Xia, *Science* **2009**, *324*, 1302–1305; n) F. Wang, Y. Han, C. S. Lim, Y. H. Lu, J. Wang, J. Xu, H. Y. Chen, C. Zhang, M. H. Hong, X. G. Liu, *Nature* **2010**, *463*, 1061–1065.

[5] a) C. J. Murphy, T. K. San, A. M. Gole, C. J. Orendorff, J. X. Gao, L. Gou, S. E. Hunyadi, T. Li, *J. Phys. Chem. B* **2005**, *109*, 13857–13870; b) B. Nikoobakht, M. A. El-Sayed, *Chem. Mater.* **2003**, *15*, 1957–1962; c) Y. G. Sun, B. Gates, B. Mayers, Y. N. Xia, *Nano Lett.* **2002**, *2*, 165–168.

[6] a) C. Lofton, W. Sigmund, *Adv. Funct. Mater.* **2005**, *15*, 1197–1208; b) J. E. Millstone, G. S. Metraux, C. A. Mirkin, *Adv. Funct. Mater.* **2006**, *16*, 1209–1214.

[7] a) J. Zeng, X. Xia, M. Rycenga, P. Henneghan, Q. Li, Y. Xia, *Angew. Chem.* **2011**, *123*, 258 – 263; *Angew. Chem. Int. Ed.* **2011**, *50*, 244 – 249; b) S. H. Chen, D. L. Carroll, *Nano Lett.* **2002**, *2*, 1003 – 1007.

[8] a) L. M. Demers, M. Östblom, H. Zhang, N.-H. Jang, B. Liedberg, C. A. Mirkin, *J. Am. Chem. Soc.* **2002**, *124*, 11248 – 11249; b) M. Östblom, B. Liedberg, L. M. Demers, C. A. Mirkin, *J. Phys. Chem. B* **2005**, *109*, 15150 – 15160; c) N. H. Jang, *Bull. Korean Chem. Soc.* **2002**, *23*, 1790 – 1800.

[9] a) B. D. Chithrani, A. A. Ghazani, W. C. W. Chan, *Nano Lett.* **2006**, *6*, 662 – 668; b) C. G. Khoury, T. Vo-Dinh, *J. Phys. Chem. C* **2008**, *112*, 18849 – 18859; c) P. S. Kumar, I. Pastoriza-Santos, B. Rodriguez-Gonzalez, F. J. Garcia de Abajo, L. M. Liz-Marzan, *Nanotechnology* **2008**, *19*, 015606.

